Laboratory and Balloon Flight Performance of the Liquid Xenon Gamma Ray Imaging Telescope (LXeGRIT)

Alessandro Curioni

Submitted in partial fulfillment of the
requirements for the degree
of Doctor of Philosophy
in the Graduate School of Arts and Sciences

COLUMBIA UNIVERSITY
2004

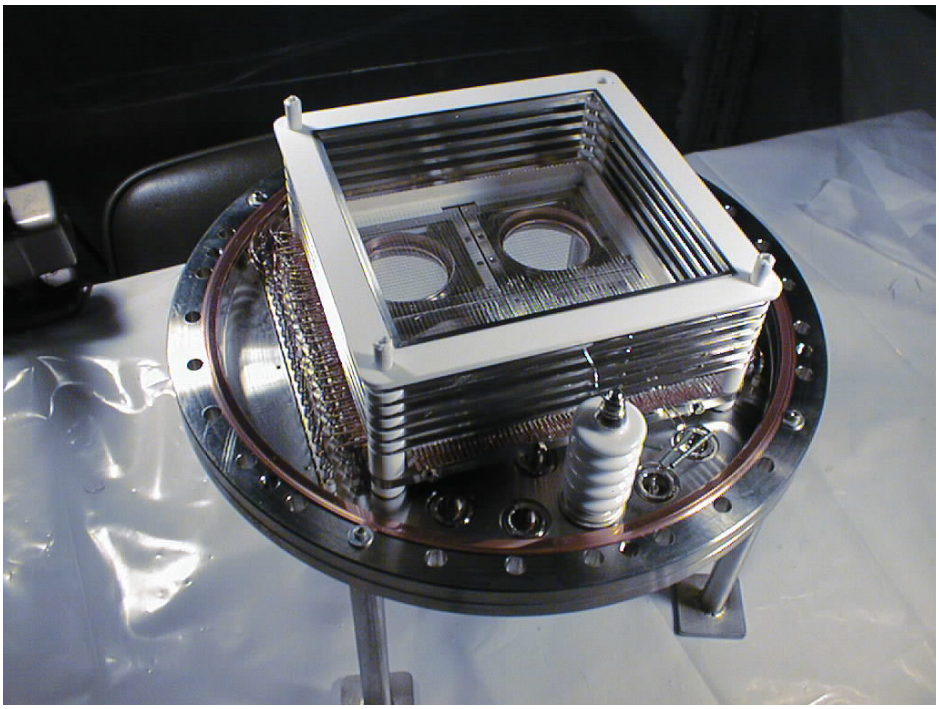

Figure 2.3: Top view of the LXeTPC with the field-shaping rings. The ceramic HV feedthrough is visible in the lower part of the picture.

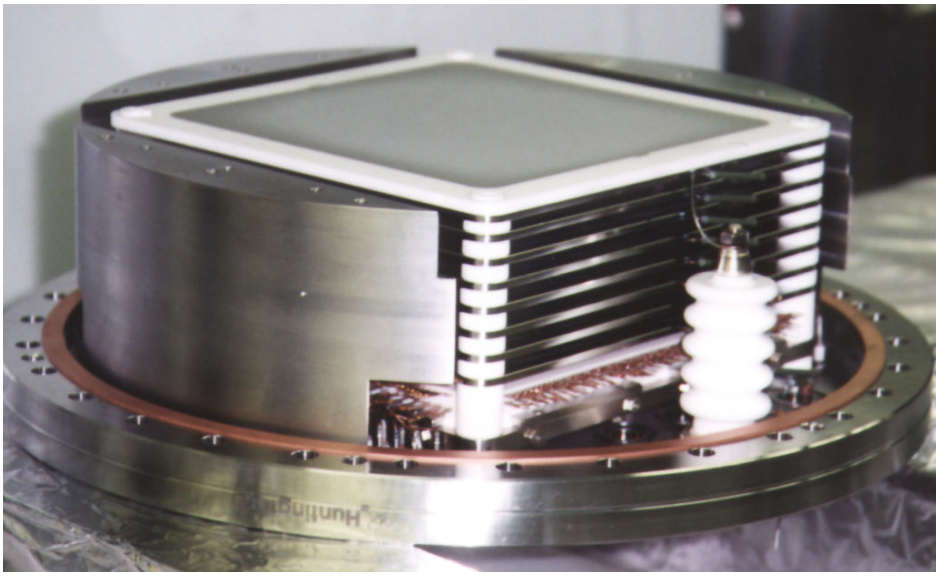

Figure 2.4: The LXeTPC completely assembled; on top, the cathode. On three sides, stainless steel spacers; on the side, the HV feedthrough.

liquid with a flow of LN_2 gas through the condenser. Since the LN_2 cooling produces microphonic noise, the vapor pressure is allowed to build up from (typically) 1.4 and 2.4 atm; at this point a solenoid valve opens to start the flow of LN_2 and it closes once the pressure reaches again 1.4 atm. An example of such a cycle is shown in Fig. 2.5, as pressure of Xe vapor vs. time.

2.1.3 LXe purification

It is well known that for detectors with a large drift region, like LXeGRIT, the Xe purity plays a major role in determining the charge yield and thus the spectral response. The most common electro-negative impurities dissolved in LXe which affect the drift of free electron are O_2, H_2O, CO, CO_2 and N_2O. The level of contamination must be kept lower than 1 ppb O_2 equivalent. To do so, an efficient purification system capable of purifying several liters of LXe was developed. The Xe gas purification and handling system for the LXeTPC was built based on the system used for a 3.5 liter gridded ionization chamber, fully discussed in Refs. (12) and (98). Two gas storage cylinders, each with a volume of four gallons, are used to store LXe up to ∼30 liters.

LXe is purified through two purifiers: *i*. an Oxisorb, which removes impu-

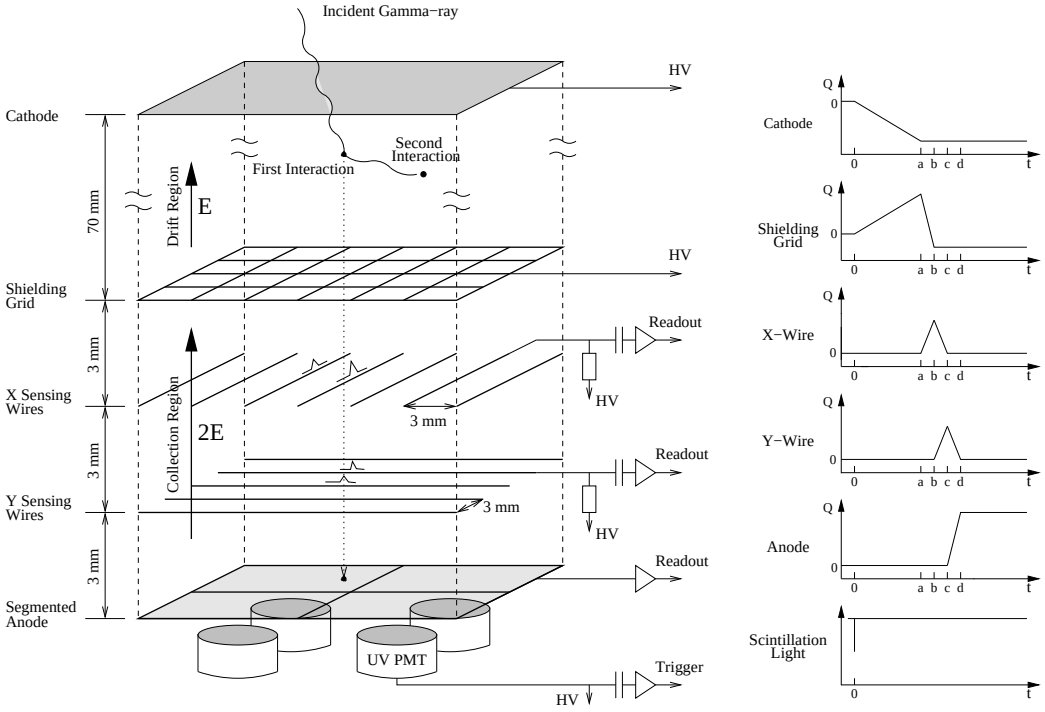

Figure 2.6: Schematic of the LXeTPC read-out structure with corresponding light trigger and charge signals (from (98) and (74)).

detection efficiency for energy deposits of $\sim$ 100 keVis near 100%.

The display of a *raw event* is shown in Fig. 2.9. It consists of the FADC pulse height signals of 62 x-wires, 62 y-wires and 2 anodes, out of 4, where a signal has been detected, all of them plotted vs. drift time, which constitutes the z-axis. The size of such an event is $\sim$30 kB. The more usual data-taking mode transfers only wire waveforms which crossed preset thresholds together with the four anode waveforms. For typical settings, the average event-size is $\sim$5 kB.

2.1.6 Data acquisition

This section is adapted from Ref. (10).

in the energy peaks. Fig. 3.19-*right* separately shows the 1-site and the multi-site energy spectra. The double-escape peak is very prominent in the 1-site spectrum, while the full energy peak goes almost undetected. The efficiency for containment is much enhanced in multi-site spectrum.

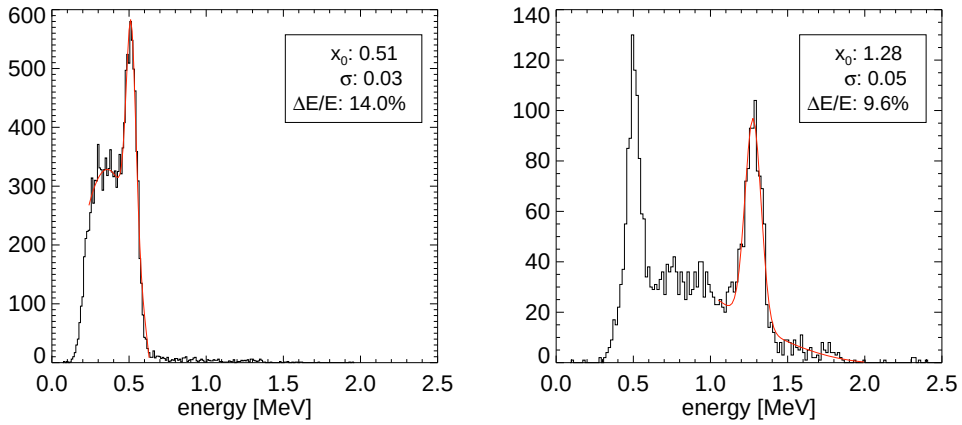

Figure 2.26: *Left:* 0.511 MeV line from a ^{22}Na source tagged source, 1-site events. The spectrum has been fitted fitted with a gaussian plus a second order polynomial to account for the underlying background; the mean and r.m.s. of the gaussian are shown in the inlet, together with the ΔE/E (FWHM). *Right:* 0.511 MeV and 1.275 MeV lines from a ^{22}Na source source, 2-site events.

Energy resolution and calibration

The starting point for the energy calibration are the energy spectra for 1-site events and the lines used for calibration are given in Table 2.1. In 1999 2-site events from ^{88}Y (single escape peak) and Am-Be 2-site and 3-site events have been used too. Each of the four anodes is independently calibrated. Each line is fitted with a gaussian plus a second order polynomial to account for the underlying background and the line position and spread come from the mean and variance of the gaussian. Several examples of such a procedure are shown in Figs. 2.26 - 2.28. This procedure could not be applied in the cases of ^{88}Y single escape peak, Am-Be single escape peak and Am-Be Compton edge,

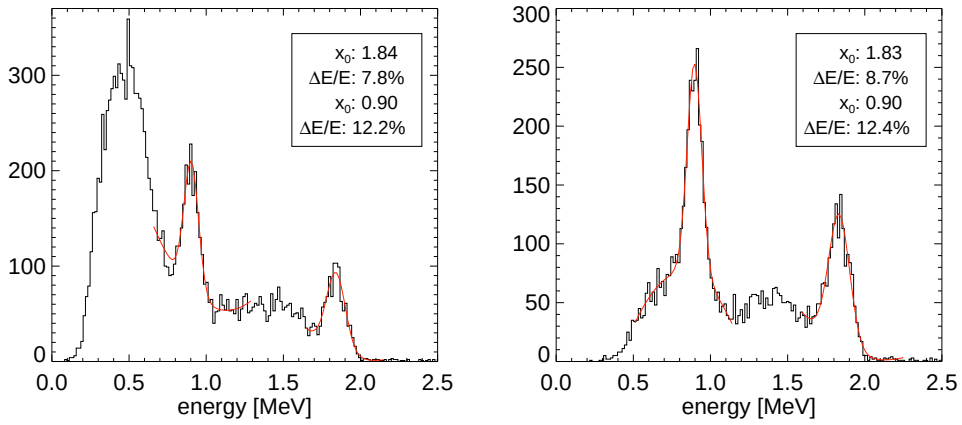

Figure 2.27: ^{88}Y (0.898 and 1.836 MeV) 1-site (*left*) and 2-site (*right*) energy spectra.

because the "line profile" was not well reproduced by a gaussian. In these cases the maximum was used instead of the mean of the gaussian, bypassing the fitting procedure.

The energy calibration, i.e. finding the conversion factors from ADC ch. to MeV, is readily obtained, showing a very good linearity in the 0.5-4.5 MeV energy range. For multi-site events, the amplitude associated with each interaction is transformed from ADC ch. to MeV according to the 1-site calibration, and the total energy is then found summing up the various interactions. This is important for LXeGRIT, because not only the total energy is needed but also the energy for each interaction. This procedure works well and line energies for 1-site and multi-site events coincide within uncertainties, i.e. better than 1%.

The energy resolution is then obtained using the same lines, but excluding the ones not reproducible through the gaussian fit; the ^{60}Co doublet has also been excluded, because of limited statistics.

The energy dependence of the energy resolution was then fitted using

$$\Delta E/E(FWHM) \;=\; \sqrt{\frac{P_1^2}{E} + \frac{P_2}{E^2}}$$

where P_1 accounts for the intrinsic energy resolution which should come from the statistics of charge carriers in LXe and should account for the $1/\sqrt{E}$